Effects of Membrane Thickness and Heat Treatment on the Gas Transport Properties of Membranes Based on P84 Polyimide

Yi Shen, Aik Chong Lua

School of Mechanical and Aerospace Engineering, Nanyang Technological University, Singapore 639798, Republic of Singapore

Received 20 July 2009; accepted 17 November 2009
DOI 10.1002/app.31810
Published online 28 January 2010 in Wiley InterScience (www.interscience.wiley.com).

ABSTRACT: P84 polyimide membranes with thicknesses ranging from 6 to 310 μm were successfully fabricated by spin coating. The glass transition temperature of the P84 powder was found to be 315°C using differential scanning calorimetry, whereas its decomposition temperature was 536°C using thermogravimetric analysis. Scanning electron microscopy was used to examine the morphology of the membranes. The permeability of single gas (He, N_2, O_2, and CO_2) and the ideal selectivity of gas pair (O_2/N_2, He/CO_2, CO_2/N_2, and He/O_2), as a function of membrane thickness, were determined. The results showed that the permeability of a single gas increased with increasing membrane thickness, whereas the selectivity of a given gas pair was nearly independent of the membrane thickness. The average selectivity of O_2/N_2, He/CO_2, CO_2/N_2, and He/O_2 were found to be 8.2, 10.0, 12.9, and 15.8, respectively. The effects of heat treatment on the membrane morphology and gas transport properties were investigated for three annealing temperatures, i.e., 80°C, 200°C, and 315°C. The membrane annealed at 315°C was cracked due to the stress sustained either during heating or cooling, thereby resulting in little or no selectivity. The permeabilities of P84-118 membrane (118 μm thickness) annealed at 80°C were 16.2, 0.196, 1.20, and 2.01 Barrer for He, N_2, O_2, and CO_2, respectively. The permeabilities of P84-118 membrane annealed at 200°C decreased by 9.75%, 47.96%, 25.83%, and 30.85% for He, N_2, O_2, and CO_2, respectively, as compared with those at 80°C, whereas the ideal selectivities increased by 42.65%, 30.52%, 32.85%, and 21.63% for O_2/N_2, He/CO_2, CO_2/N_2, and He/O_2, respectively. J Appl Polym Sci 116: 2906–2912, 2010

Key words: P84 co-polyimide; membrane thickness; gas separation; heat treatment; permeability

INTRODUCTION

Polymeric membranes have been of great interest in the food production industry[1] and in the separation of many important industrial gases, such as oxygen/nitrogen enriched air, hydrogen recovery from purge steam in ammonia plants or hydrogenation processes, natural gas dehydration, and hydrocarbon recovery.[2–4] Such interest in polymeric membrane technology is due to the easy processability of membranes and low capital investment cost. Glassy polymers that have lower intrasegmental mobility and longer relaxation time are always preferentially chosen as practical membrane materials, amongst the various polymer materials, for gas separation because of their inherent high selectivity, excellent thermal and chemical stability, and good mechanical properties.

Recently, to further enhance membrane performance for gas separation, considerable work has focused on exploring new membrane materials[5,6] and novel membrane structure designs.[7–10] For practical applications, membrane thickness also plays a critical role in gas separation performance and cost-effective productivity. To the best of the authors' knowledge, limited work is devoted to investigating the effect of membrane thickness on the transport properties of membranes. Yang et al.[11] investigated the water sorption and diffusion behavior of Kapton films with different thicknesses and found that the water diffusivity in the 50 μm film was three times larger than that in the 7.5 μm film due to the difference in the molecular aggregate orientation. Mensitieri et al.[12] investigated the effect of film thickness on oxygen sorption and diffusion in Kapton® polyimide. They observed sharp increases in permeability, solubility, and diffusivity coefficient for increasing film thickness for 13–50 μm range. Koops et al.[13] studied the pervaporation selectivity as a function of the membrane thickness and found the selectivity of polysulfone (PSF), poly(vinyl chloride) (PVC), and polyacrylonitrile (PAN) decreased with decreasing membrane thickness, below a limiting value of about 15 μm. Huang and Paul[14] investigated the relationship between the physical aging and film thickness. They found that the resulting films exhibited a distinct decrease in permeability with time due to

Correspondence to: A. C. Lua (maclua@ntu.edu.sg).

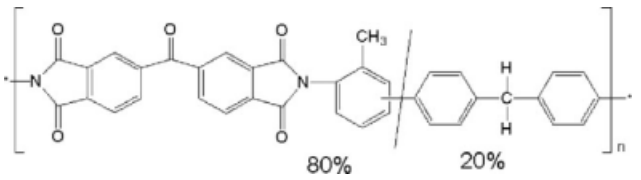

Figure 1 Chemical structure of P84 (BTDA-Me4PDA/MDA) co-polyimide.

physical aging, and the physical aging effect became greater for the thinner films.

P84 co-polyimide (BTDA-Me4PDA/MDA, co-polyimide of 3,3′,4,4′-benzophenone tetracarboxylic dianhydride and 80% methylphenylene-diamine + 20% methylene diamine), a commercially available glassy polymer, has attracted significant attention as a novel membrane material for gas separation[15–21] and pervaporation[22–27] due to its high selectivity with superior anti-plasticization properties against CO_2. In this study, P84 co-polyimide membranes of thicknesses ranging from 5 to 310 μm were prepared by spin coating. The effect of membrane thickness on gas permeability and selectivity and the effect of heat treatment on membrane properties were investigated.

EXPERIMENTAL

DSC and TGA characterizations of P84 polymer powder

P84 co-polyimide powder for preparing the membranes was supplied by HP Polymer GmbH, Austria. The chemical structure of P84 co-polyimide is shown in Figure 1. To investigate the thermal stability of the P84 polyimide, a thermogravimetric analyzer (TGA 7, PerkinElmer) was used. The thermogravimetric analysis (TGA) was operated at a temperature range of 25–900°C using a heating rate of 20°C/min under nitrogen atmosphere. A differential scanning calorimeter (DSC 7 Sub-Amb, PerkinElmer) was used to determine the glass transition temperature (T_g) of the P84 polyimide. The DSC tests were conducted at a temperature range of −20°C to 400°C using a heating rate of 20°C/min.

Fabrication of P84 membranes with various thicknesses

The P84 powder was degassed under vacuum at 373°C overnight to remove any moisture before the preparation of the membranes. A total of 8 g of P84 powder was dissolved in 20 mL of *N*-methyl-2-pyrrolidinone and the mixture was stirred at 60°C for three days. The solution was then cooled to ambient temperature and left standing for several hours to remove any gas bubbles before spin coating.

A spincoater (Model P6700, Specialty Coating Systems) was used to prepare the membranes with various thicknesses by varying the number of coats. During spin coating, two types of substrates, i.e., porous stainless steel substrates and poly(methyl methacrylate) (PMMA) substrates were used to prepare defects-free membranes with thicknesses ranging from 6 to 310 μm. Before spin coating, the porous stainless steel substrates were ultrasonic-cleaned in ethanol for 5 min and rinsed with ethanol for several times to remove any surface contaminants. They were then immersed into a solution of 2 wt % cetyltrimethylammonium bromide (C_{16}TAB) and ethanol for 10 min and rinsed with ethanol thrice. Finally, they were dried in an oven at 100°C overnight. For the PMMA substrates, they were cleaned with ethanol but without immersing into a solution of C_{16}TAB and ethanol, and then dried at 60°C in an oven overnight.

During its operation, the spin coating system was evacuated by a vacuum pump and the working chamber was purged by a stream of nitrogen gas to ensure an inert condition. All the spin coatings were conducted under ambient temperature. The process parameters for the spin coating are shown in Table I. During each spin coating, 0.4 mL P84 solution was injected onto the substrate with a syringe. After each coating, the substrate together with the coating membrane was taken from the spincoater and dried in a vacuum oven under ambient temperature. The thicknesses of the coating membranes were varied by the number of separate coats applied.

Heat treatment of P84 membranes

To study the effects of heat treatment on the morphology and gas transport properties of the membranes, membranes with thickness of 118 μm were annealed under vacuum at three different temperatures, i.e., 80°C, 200°C, and 315°C. For the annealing temperatures of 80°C and 200°C, it was conducted using a vacuum oven (C3000, France Etuves), whereas for that at 315°C, the annealing was conducted using a furnace (Eurotherm 2416CG, Carbolite) with a temperature controller. For each annealing process, the temperature was increased at the rate of 0.5°C/min to the preset temperature and kept at that temperature for 24 h. Finally, the samples were cooled down to room temperature at the same rate.

TABLE I
Process Parameters for Spin Coating

Stage	1	2	3	4
Speed (rpm)	1000	2000	6000	0
Ramp (s)	5	5	10	10
Time (s)	10	10	20	–

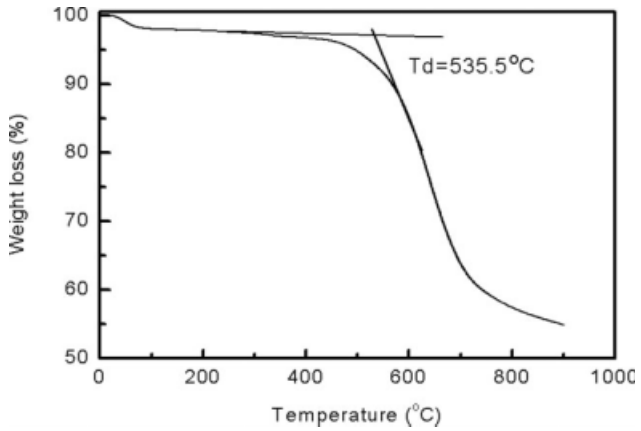

Figure 2 Thermogravimetric analysis curve of P84 powder.

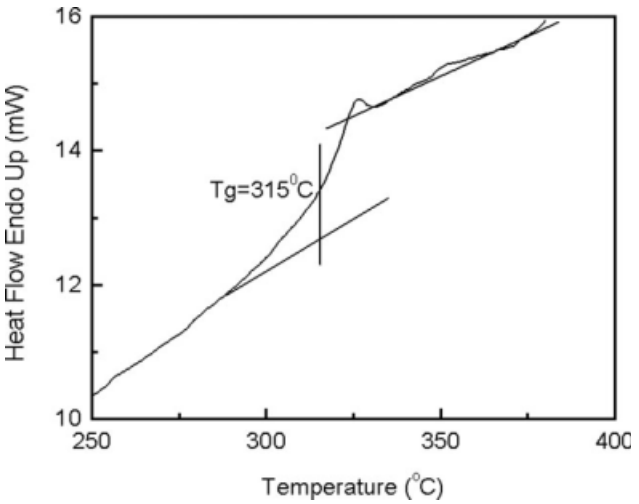

Figure 3 Differential scanning calorimetry curve of P84 powder.

Scanning electron microscopy

Scanning electron microscopy (JSM-5600LV, JEOL) was used to examine the morphology of the resulting membranes. Before the scans, all the samples were coated with platinum. For the cross-sectional views, the samples were attached to a vertical surface and then coated with platinum.

Permeation measurements

Single gas permeation tests on the P84 membranes were conducted using a constant volume, varying pressure experimental set-up as described in Lua and Su.[28] The single gas used in these tests was He, N_2, O_2, and CO_2. Each gas was of a purity of 99.99%. All the tests were carried out at room temperature. Once the membranes were prepared, they were not left standing but subjected to permeation tests. Hence, the effect of aging, if any, would be insignificant for all the membranes tested. The gas permeability P was determined in accordance to that given by Cong et al.[29] and its unit is in Barrer (1 Barrer $= 1 \times 10^{-10}$ cm^3 (STP) cm/(cm^2 s cmHg)). The permeability P is given by

$$P = \frac{VL}{ART\Delta P}\frac{dp}{dt}$$

where V is the downstream volume, L is the membrane thickness, A is the effective membrane area, R is the universal gas constant, T is the absolute temperature, ΔP is the transmembrane pressure difference $p_1 - p_2$ (where p_1 and p_2 are the upstream and downstream pressures, respectively), and dp/dt is the steady rate at which the pressure is increasing on the downstream side. To determine the performance of the membrane per unit thickness basis, the membrane permeance $\overline{P}(\overline{P} = P/L)$ is used and is defined as the ratio of permeability P to membrane thickness L. The ideal selectivity S of a given gas pair is given by

$$S = P_A/P_B$$

where P_A and P_B are the permeabilities of single gases A and B, respectively. Membrane coated on the porous stainless steel substrate was used directly for the gas permeation test, whereas membrane coated on PMMA substrate was peeled from the substrate and then assembled into the gas permeation set-up. The thickness of membrane was measured by a micrometer. For each membrane, eight measurements on different locations were conducted and the average value was obtained.

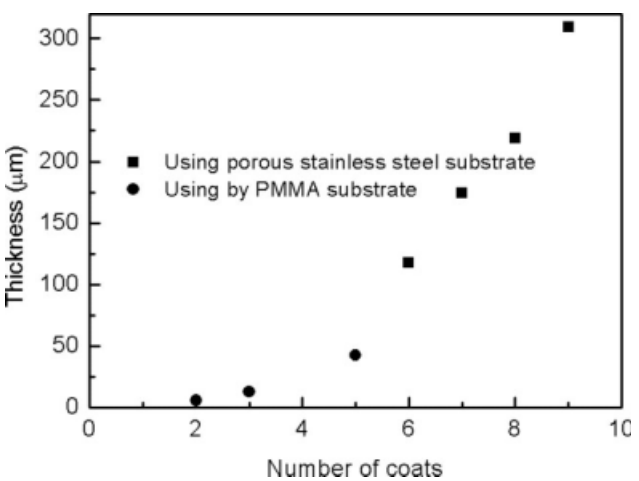

Figure 4 Relationship between the membrane thickness and the number of coats using porous stainless steel and PMMA substrates.

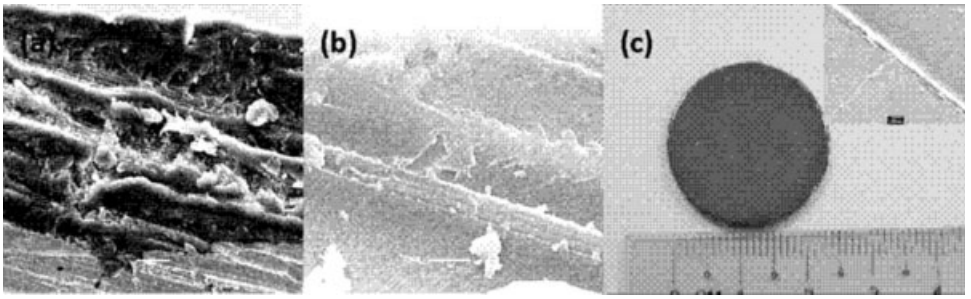

Figure 5 SEM micrographs of the cross-section of P84-118 membrane annealed at (a) 80°C, and (b) 200°C, and (c) a digital photograph together with the SEM micrograph of top surface (insert) of P84-118 annealed at 315°C.

RESULTS AND DISCUSSION

TGA and DSC results

Figures 2 and 3 show the TGA and the DSC curves of the P84 powder, respectively. From the TGA curve, the decomposition temperature of P84 powder was 535.5°C, indicating its excellent thermal stability. A weight loss of about 4% at the temperature of 100°C was due to the moisture present in the powder. The glass transition temperature of P84 as determined from the DSC curve was 315°C, which was consistent to that reported by Qiao et al.[24]

P84 membranes with various thicknesses

For the preparation of the membrane, porous stainless steel substrates were initially used because of the ease in processing the membranes for the gas permeation tests. However, it was difficult to obtain defects-free membranes with thickness <50 μm using these substrates. Dense PMMA substrates with much smoother surface were subsequently used for preparing thinner membranes. The membrane prepared using PMMA substrate had to be detached from the substrate by immersing it into ethanol/water solution. A total of seven membranes with thickness ranging from 6 to 310 μm were prepared by controlling the number of spinning coats. The relationship between the membrane thickness and the number of coats is shown in Figure 4. The membrane with a certain thickness L was labeled as "P84-L." For example, a membrane with thickness of 309 μm was labeled as P84-309.

Effect of heat treatment on the properties of P84 membranes

The study on the effect of heat treatment on the P84 membranes was carried out on the membranes having a thickness of 118 μm. Membrane P84-118 was annealed at three different temperatures, i.e., 80°C, 200°C, and 315°C, to investigate the effect of heat treatment on its gas transport properties. Membranes annealed at 315°C were found to be cracked due to the unequal thermal stress generated at the interface between the substrate and the polymer membrane during the heating or cooling process. The membrane had a line crack as shown in Figure 5(c), whereas the membranes annealed at 80°C and 200°C were defects-free. Table II shows that P84-118 membrane annealed at 200°C yields higher selectivity than that at 80°C, but lower permeability for all the single gas (He, N_2, O_2, and CO_2). The permeabilities of P84-118 annealed at 80°C are 16.2, 0.196, 1.20, and 2.01 Barrer for He, N_2, O_2, and CO_2, respectively. The permeabilities of P84-118 membrane annealed at 200°C decreased by 9.75%, 47.96%, 25.83%, and 30.85% for He, N_2, O_2, and CO_2, respectively, as compared with those at 80°C, whereas the ideal selectivities increased by 42.65%, 30.52%, 32.85%, and 21.63% for O_2/N_2, He/CO_2, CO_2/N_2, and He/O_2, respectively. This behavior of gas transport in P84-118 membranes was due to the different membrane morphologies, resulting from different annealing temperatures. As shown in Figure 5(a), there was a distinct lamination structure in the cross-section of P84-118 membrane annealed at 80°C, which was formed due to the separate layers of coating. For the membrane P84-118 annealed at 200°C,

TABLE II
Transport Properties of P84-118 Membrane Annealed at 80°C and 200°C

	Permeability P (Barrer)				Selectivity S			
Temperature (°C)	He	N_2	O_2	CO_2	O_2/N_2	He/CO_2	CO_2/N_2	He/O_2
80	16.2	0.196	1.20	2.01	6.12	8.06	10.26	13.50
200	14.62	0.102	0.89	1.39	8.73	10.52	13.63	16.42

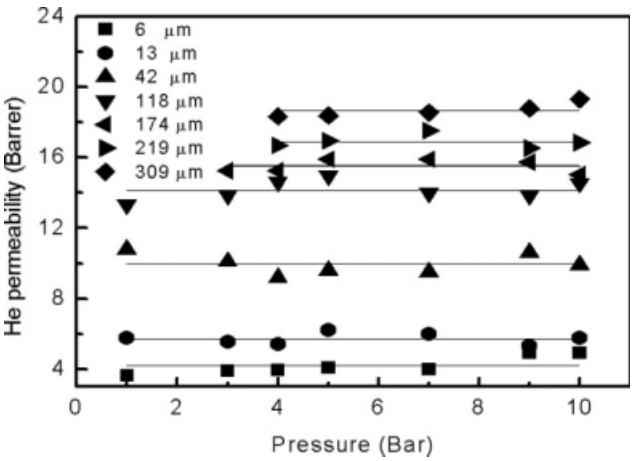

Figure 6 Permeability of helium for various membranes subjected to different feed pressures.

the different layers of polymer were sintered together and the lamination lines disappeared due to chain movements as shown in Figure 5(b). This is reasonable considering the fact that a higher temperature is favorable to chain movements in polymers. This is termed the densification process whereby the excess free volume of the membranes is reduced. This, in turn, enhances selectivity but reduces permeability of the membrane. Subsequently, to ensure good performance in gas separation, all membranes were prepared and annealed at 200°C.

Effect of membrane thickness on gas transport properties of P84 membranes

Gas permeation tests were carried out to investigate the effect of membrane thickness on the transport properties of P84 membranes. Figure 6 shows that the helium permeability through membranes with different thicknesses (P84-6 to P84-309) is independent of pressure. This behavior is characteristic of the permeation of nonplasticizing gases through glassy polymers and also indicates that some nonselective transport mechanisms, such as Knudsen flow, are not present during the gas transport processes. Further, there were no defects or pinholes present in the membranes as verified by the SEM micrographs obtained, but not presented in this article.

The gas permeation results for helium, nitrogen, oxygen, and carbon dioxide and the ideal selectivity of the given gas pairs are shown in Table III. A feed pressure of 4 bars was used for all the tests. For all the single gases (He, N_2, O_2, and CO_2), their permeabilities are highly dependent on the membrane thickness whereby the permeability increases with increasing membrane thickness. The permeability of all the single gases increased by more than three times as the membrane thickness increased from 6 to 309 μm. Table III also shows that the permeability of the single gas increases in the following order: He (2.6 Å) > CO_2 (3.3 Å) > O_2 (3.46 Å) > N_2 (3.64 Å), with its respective molecular gas diameter given within the parenthesis. These trends are also shown in Figure 7. Hence, the permeability of the gas increases with decreasing size of the gas molecule, as expected. P84 is a partial crystallized polyimide and its crystallinity level, crystallinity orientation, and excess free volume are highly dependent on the membrane thickness.[30] Thinner membranes have a lower crystallinity level, smaller excess free volume, and a higher molecule chain alignment in a parallel orientation to the membrane surface. These membrane structure and morphology have considerable influences on the gas transport properties through the membrane. Lower crystallinity will lead to increased gas permeability but smaller excess free volume and higher molecule chain alignment will both lead to decreased gas permeability due to increased pore diffusion resistance. Of the four single gases studied in this work, Figure 7 shows that the permeability of each single gas decreases with decreasing membrane thickness. For a thinner membrane, the combined effects of a smaller excess free volume and a higher molecule chain alignment in a parallel orientation to the membrane surface are more pronounced than the lower crystallinity effect and, therefore, result in lower permeability as compared with a thicker membrane. The numerical values of permeability for the various single gases for different membrane thicknesses are given in

TABLE III
Single Gas Permeability and Selectivity of Gas Pairs for Membranes with Various Thicknesses

	Permeability P (Barrer)				Selectivity S			
Thickness L (μm)	He	N_2	O_2	CO_2	O_2/N_2	He/CO_2	CO_2/N_2	He/O_2
6	4.02	0.039	0.26	0.41	6.67	9.66	10.51	15.23
13	5.41	0.051	0.36	0.59	7.06	9.19	11.57	15.06
42	9.20	0.065	0.57	0.92	8.77	10.0	14.16	16.14
118	14.64	0.102	0.89	1.39	8.73	10.52	13.63	16.42
174	15.31	0.117	0.95	1.48	8.12	10.32	12.65	16.07
219	17.09	0.122	1.09	1.66	8.93	10.27	13.61	15.56
309	18.33	0.127	1.13	1.82	8.90	10.06	14.33	16.20

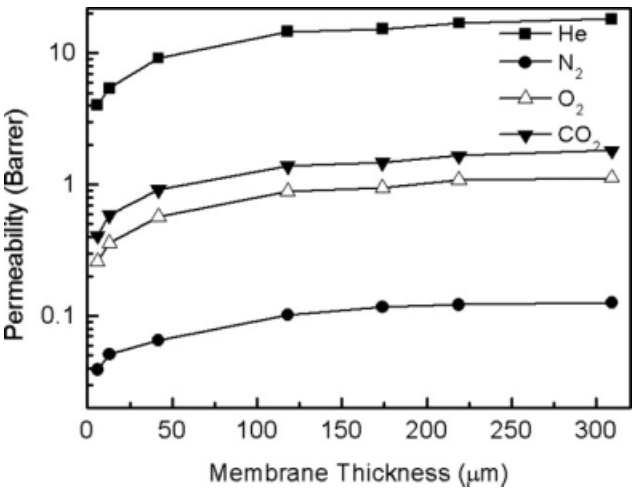

Figure 7 Permeability of membranes with various thicknesses.

Table III. The effect of aging on the gas permeability is probably negligible as all the P84 membranes were used soon after they were prepared. To further evaluate the gas permeability through the membranes with varying thicknesses, the relationship between the permeance and the membrane thickness is shown in Figure 8 and Table IV. The permeance of single gas (He, N_2, O_2, and CO_2) decreases with increasing membrane thickness. This is due to the fact that the pore diffusion resistance through the membrane increases exponentially with increasing membrane thickness due to increasing tortuosity effects, resulting in increasing gas path length. The selectivity of gas pairs (O_2/N_2, He/CO_2, CO_2/N_2, and He/O_2) seems to be almost independent of membrane thickness as shown in Figure 9, although some minor variations could be observed. Such relationship between selectivity and membrane thickness was also reported for other polymer materials,

TABLE IV
Single Gas Permeance for Membranes with Various Thicknesses

Thickness L (μm)	Permeance $\overline{P}$ (Barrer/μm)			
	He	N_2	O_2	CO_2
6	0.6700	0.0065	0.0433	0.0683
13	0.4162	0.0039	0.0277	0.0454
42	0.2191	0.0015	0.0136	0.0219
118	0.1241	0.0009	0.0075	0.0118
174	0.0880	0.0007	0.0055	0.0085
219	0.0780	0.0006	0.0050	0.0076
309	0.0593	0.0004	0.0037	0.0059

such as polysulfone (PSF), polyetherimide, and polycarbonate.[13] From Table III, the average selectivity of O_2/N_2, He/CO_2, CO_2/N_2, and He/O_2 were found to be about 8.2, 10.0, 12.9, and 15.8, respectively.

CONCLUSIONS

P84 polyimide membranes with thicknesses ranging from 6 to 310 μm were fabricated by spin coating. The effects of heat treatment on the membrane morphology and gas transport properties were investigated. It was found that membrane P84-118 (118 μm thickness) annealed at 315°C for 24 h, cracked because of the stress generated in the interface between the substrate and the polymer membrane, resulting in very low or no selectivity. Membrane P84-118 annealed at 200°C exhibited higher selectivity but lower permeability than that annealed at 80°C. The permeabilities of P84-118 annealed at 80°C are 16.2, 0.196, 1.20, and 2.01 Barrer for He, N_2, O_2, and CO_2, respectively. The permeabilities of P84-118 membrane annealed at 200°C decreased by 9.75%, 47.96%, 25.83%, and 30.85% for He, N_2, O_2, and CO_2, respectively, as compared with those at 80°C,

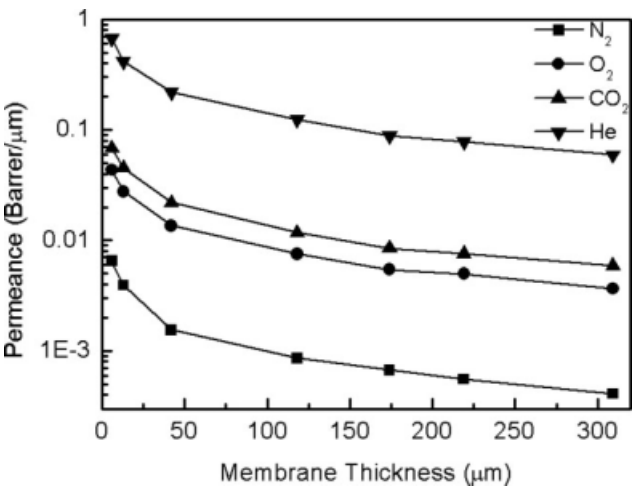

Figure 8 Permeance of membranes with various thicknesses.

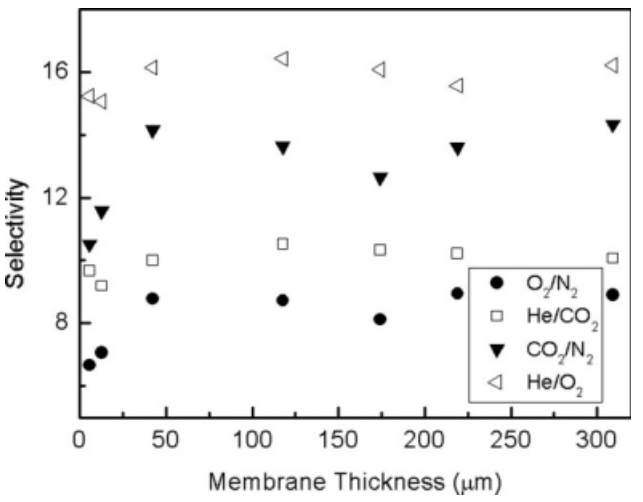

Figure 9 Selectivity of membranes with various thicknesses.

whereas the ideal selectivities increased by 42.65%, 30.52%, 32.85%, and 21.63% for O_2/N_2, He/CO_2, CO_2/N_2, and He/O_2, respectively. The SEM micrographs revealed that the higher annealing temperature of 200°C was favorable to fuse the lamination lines resulting from the separate coats during preparation, and this could reduce excess free volume and densify the membrane. The helium permeability for the membranes with varying thicknesses was found to be independent of the feed pressure, indicating the absence of defects or pinholes in the membranes. The gas permeation tests showed that the permeability of membranes increased significantly with increasing membrane thickness. This is due to the combined effects of larger excess free volume and lower molecular chain alignment in a parallel orientation to the membrane surface, which predominate over the adverse effect of higher crystallinity level in a thicker membrane. The selectivity of gas pairs was nearly independent of the variations in membrane thickness.

References

1. Psomiadou, E.; Arvanitoyannis, I. S.; Biliaderis, C. G.; Ogawa, H.; Kawasaki, N. Carbohydr Polym 1997, 33, 227.
2. Spillman, R. W. Chem Eng Prog 1989, 85, 41.
3. Ghosal, K.; Freeman, B. D. Polym Adv Technol 1994, 5, 673.
4. Koros, W. J.; Fleming, G. K. J Membr Sci 1993, 83, 1.
5. Stern, S. A. J Membr Sci 1994, 94, 1.
6. Hensema, E. R. Adv Mater 1994, 6, 269.
7. Maier, G. Angew Chem Int Ed Engl 1998, 37, 2960.
8. Pinnau, I. Polym Adv Technol 1994, 5, 733.
9. Abetz, V.; Brikmann, T.; Dijkstra, M.; Ebert, K.; Frithch, D.; Ohlrogge, K.; Paul, D.; Peinemann, K. V.; Nunes, S. P.; Scharnagl, N.; Schossig, M. Adv Eng Mater 2006, 8, 328.
10. Chung, T. S.; Jiang, L. Y.; Li, Y.; Kulprathipanja, S. Prog Polym Sci 2007, 32, 483.
11. Yang, D. K.; Koros, W. J.; Hopfenberg, H. B.; Stannett, V. T. J Appl Polym Sci 1986, 31, 1619.
12. Mensitieri, G.; Del Nobile, M. A.; Monetta, T.; Nicodemo, L.; Bellucci, F. J Membr Sci 1994, 89, 131.
13. Koops, G. H.; Nolten, J. A. M.; Mulder, M. H. V.; Smolders, C. A. J Appl Polym Sci 1994, 53, 1639.
14. Huang, Y.; Paul, D. R. Ind Eng Chem Res 2007, 46, 2342.
15. Barsema, J. N.; Kapantaidakis, G. C.; van der Vegt, N. F. A.; Koops, G. H.; Wessling, M. J Membr Sci 2003, 216, 195.
16. Bos, A.; Pünt, I.; Strathmann, H.; Wessling, M. AIChE J 2001, 47, 1088.
17. Visser, T.; Masetto, N.; Wessling, M. J Membr Sci 2007, 306, 16.
18. Visser, T.; Wessling, M. J Membr Sci 2008, 312, 84.
19. Sterescu, D. M.; Stamatialis, D. F.; Wessling, M. J Membr Sci 2008, 310, 512.
20. Li, Y.; Chung, T. S. Microporous Mesoporous Mater 2008, 113, 315.
21. Li, Y.; Chung, T. S.; Huang, Z.; Kulprathipanja, S. J Membr Sci 2006, 277, 28.
22. Wang, K. Y.; Chung, T. S.; Rajagopalan, R. J Membr Sci 2007, 287, 60.
23. Qiao, X. Y.; Chung, T. S. Ind Eng Chem Res 2005, 44, 8938.
24. Qiao, X. Y.; Chung, T. S.; Pramod, K. P. J Membr Sci 2005, 264, 176.
25. Qiao, X. Y.; Chung, T. S.; Rajagopalan, R. Chem Eng Sci 2006, 61, 6816.
26. Liu, R. X.; Qiao, X. Y.; Chung, T. S. J Membr Sci 2007, 294, 103.
27. Teoh, M. M.; Chung, T. S.; Wang, K. Y.; Guiver, M. D. Sep Purif Technol 2008, 61, 404.
28. Lua, A. C.; Su, J. C. Carbon 2006, 44, 2964.
29. Cong, H. L.; Hu, X. D.; Radosz, M.; Shen, Y. Q. Ind Eng Chem Res 2007, 46, 2567.
30. Sroog, C. E. Prog Polym Sci 1991, 16, 561.